

Elucidating the Membrane Diffusion Dynamics of Muscarinic-1 Acetylcholine Receptors with
Quantum Dots

By

Devin Taylor

Thesis

Submitted to the Faculty of the
Graduate School of Vanderbilt University
in partial fulfillment of the requirements

For the degree of

MASTER of SCIENCE

in

Chemistry

January 31, 2020

Nashville, Tennessee

Approved:

Sandra J. Rosenthal, Ph.D.

Lauren E. Buchanan, Ph.D.

Table of Contents

	Page
List of Figures.....	iii
Introduction.....	1
Experimental and Analysis Methods.....	4
Results and Discussion.....	8
Conclusion.....	19
References.....	23

List of Figures

Figure	Page
1. Crystal structure of hM1AChR from Thal D.M. et al. (2016).....	2
2. Schematic figure of GPCR signaling cascade event from Stewart A. et al. (2012).....	3
3. Experimental setup from Vijayraghavan S. et al. (2018).....	4
4. Experimental data set from Hern J.A. et al. (2010)	5
5. Schematic of quantum dot attachment to antibody from Kovton O. et al. (2018).....	6
6. Basolateral TIRF images of HEK293 Cells.....	7
7. Charts of average cluster size of hM1AChR in HEK293 Cells.....	9
8. Charts of molecular diffusion dynamics of hM1AChR in HEK293 Cells.....	10
9. Charts of radial scatter diffusion plots of hM1AChR in HEK293 Cells.....	11
10. Schematic structure of telenzepine.....	12
11. Schematic structure of IDT791.....	13
12. HEK293 Images of IDT791 Binding with no hM1AChR Transfection.....	14
13. HEK293 Images of IDT791 Binding with hM1AChR Transfection	15
14. Schematic structure of IDT794.....	16
15. HEK293 Images of IDT794 Binding with no hM1AChR Transfection	17
16. HEK293 Images of IDT794 Binding with hM1AChR Transfection	18

Introduction

The difficulty and limited options for treating mental illness has led to high interest in studying the molecular mechanisms of various transporters and receptors in the central nervous system in hopes of providing new and more effective treatment methods. A popular target in the treatment of cognitive-related diseases is the human muscarinic-1 acetylcholine receptor (hM1AChR), a prominent metabotropic class A G-protein coupled receptor (GPCR) selectively distributed in the pre-frontal cortex (PFC) of the brain.¹ As a result, proper function and regulation of the receptor is linked to higher cognitive function.² Irregularities concerning the expected physiological functions of hM1AChR lead to illnesses such as Alzheimer's disease and schizophrenia.^{3,4} Therefore, the receptor has become a promising therapeutic target in the field. Several lines of evidence suggest that the dynamic reorganization of hM1AChR in the membrane, not its endocytic trafficking, controls its spatiotemporal signaling in response to stimulation.^{5,6,7} Elucidation of these reorganization patterns have led to the rise of single particle tracking (SPT) experiments to discover multiple molecular diffusion properties of macromolecules in cellular membranes.⁸ Semiconductor-nanocrystals, known as quantum-dots (Qdots) have emerged as leading probes due to high brightness and excellent photostability. The large advantage of Qdots feature prolonged tracking periods that extend beyond that of other popular fluorescent dyes such as Cy3B and fluorescent proteins such as GFP. Due to the unique physical properties that Qdots possess, their optimization for biocompatible experimentation in extracellular in-vitro and in-vivo environments continues to push boundaries for the collection of precise dynamic characterizations of popular cellular receptors and channels.

Previous endeavors aimed to determine the crystal structure of hM1AChR (Figure 1) have proven used in detecting popular binding sites for multiple drug candidates.^{9,10} Physiological

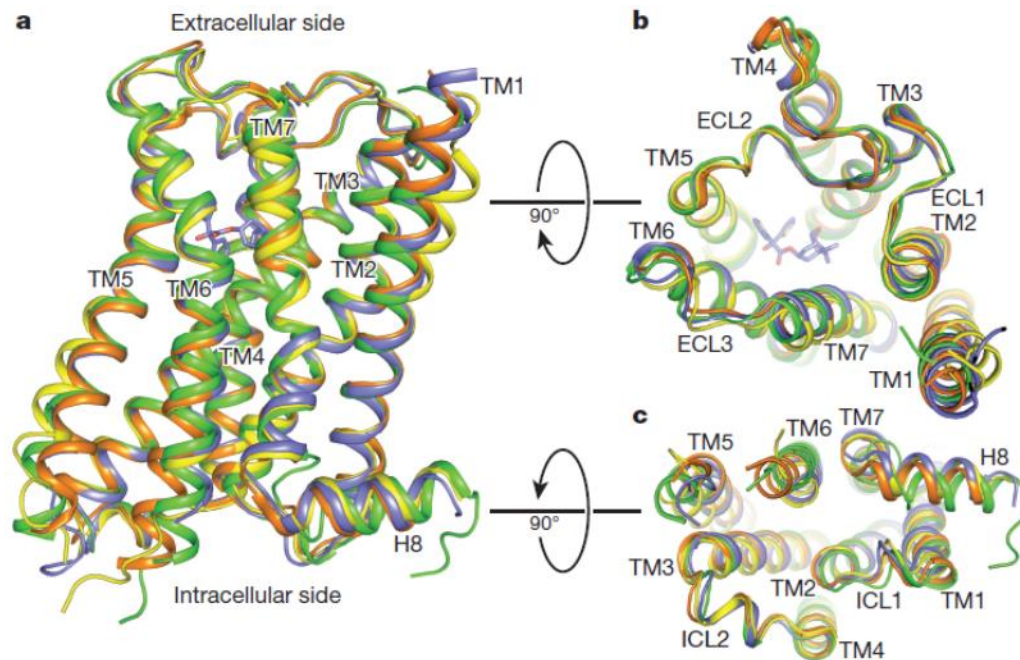


Figure 1. **Crystal structure of hM1AChR**, from Thal D.M. et al (2016)

activation of GPCRs via agonist stimulates the protein to produce a down-signaling cascade effect (Figure 2).¹¹ For hM1AChR, there have been published reports based on the molecular functions of hM1AChR post-activation aimed to discover the molecular role it plays in cellular process such as memory formation and neuronal growth.^{12,13,14}

This work is based on two primary studies that have previously examined the effects of acetylcholine activation of hM1AChR in native environments as well as a study focused on the SPT of individual hM1AChR in an in-vitro environment. The first study features an external stimulation into the brains of rhesus monkeys to regulate and maintain working memory (WM) (Figure 3).¹² The primary conclusions of this study are that while WM is easily maintained with a proper amount of acetylcholine, overstimulation will lead to degradation of this WM, an undesirable effect that undermines the regulated hM1AChR needed for proper cognitive function. In addition to these conclusions, there is still a limited understanding in the exact downstream

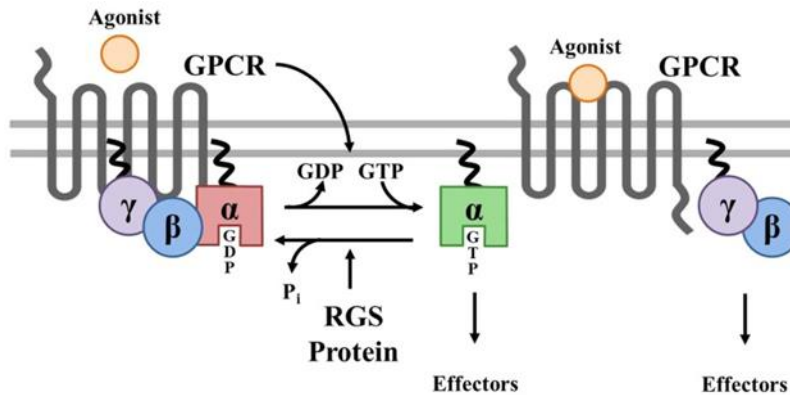


Figure 2. **GPCR downstream intracellular signaling cascade post-agonist stimulation**, from Stewart A. et al. (2012)

regulated activity of hM1AChR that are likely to assist in developing more efficient therapeutic methods in the event of unexpected mutations.

The second study cover the SPT of monomeric muscarinic-1 receptors to identify its tendency to form homodimers.¹⁵ The work done has proved to be fundamental in future SPT studies concerning a number of different GPCRs. The targeting method presented in this work used an even mix of conjugated telenzepine with Cy3B dye as well as conjugated telenzepine with Alex488. The primary results of this study show that the muscarinic-1 receptor has a 70:30 ratio of appearing in a monomer and homodimer state respectively (Figure 4). As there is direct evidence of the influence dimerization altering the structural dynamics of GPCRs such as hM1AChR, the main conclusions of this article produced one of the primary works concerning direct examination of individual proteins in the cellular membrane.^{16,17}

With building knowledge of the structural and dynamic properties of hM1AChR, the following work aims to utilize a Qdot-based probe directly attached to the extracellular N-terminus of hM1AChR for the first time. In addition, there will be data presented representing a simulated physiological environment where hM1AChR is stimulated with its native agonist, acetylcholine. Finally, an experimental approach to create new ligands based on optimal

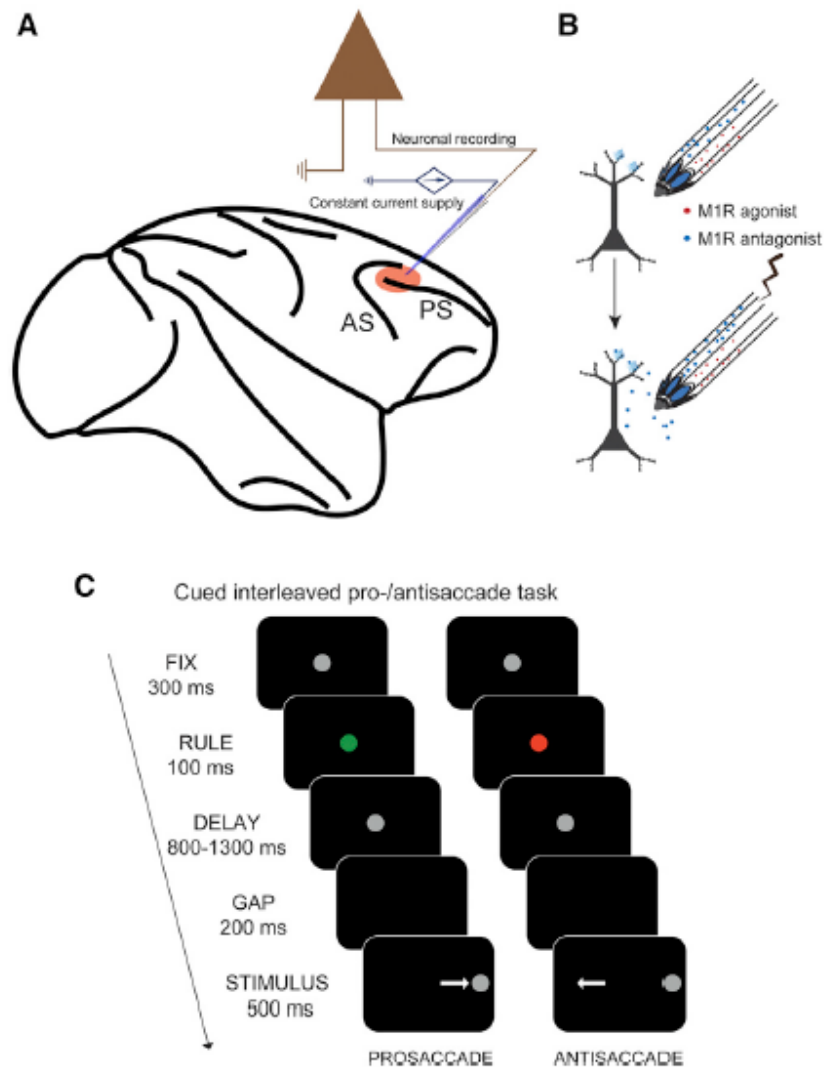


Figure 3. **Direct stimulation of M1R in neurons detects signaling directly induced through working activity either towards or away from stimulus**, from Vijayraghavan S. et al (2018)

compatibility between Qdot and cellular binding will be presented. In addition, the experiments aim determine the extent to which acetylcholine (Ach) stimulation influences hM1AChR dynamics and confinement. Ideally, new drug development strategies will emerge through the acquisition of nanoscale organizational complexity of hM1AChR. It is expected that new insights that will expand on what is currently know about hM1AChR through a targeting system that has

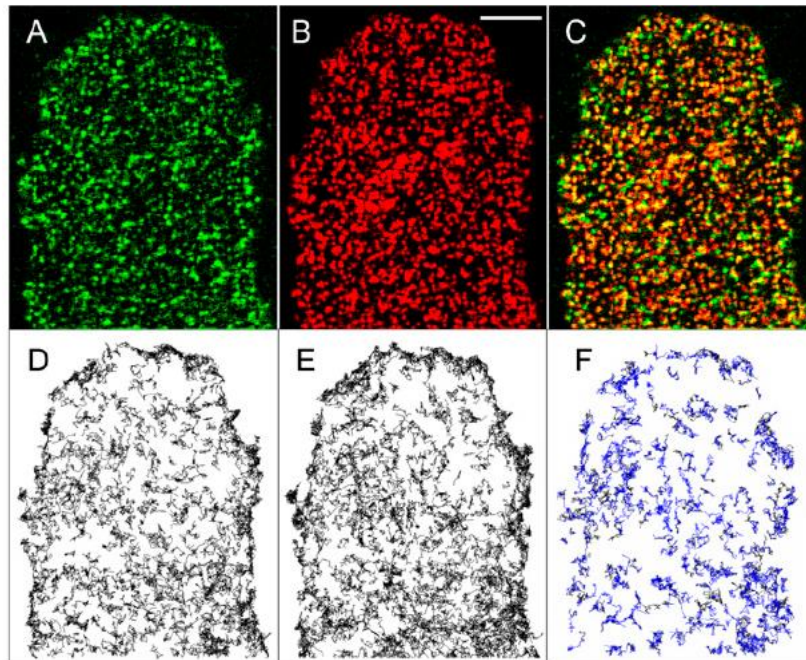


Figure 4. **Monomeric hM1AChR labeling from two fluorescent sources determine the rate in which the receptor forms dimer states**, from Hern J.A. et al (2010)

proven to be effective with other transporters and receptors.¹⁸ The ultimate goal of this report is to directly examine the influence agonist stimulation affects hM1AChR using the advantages provided by Qdots to discover new mechanisms of action for the receptor in simulated biological environments.

Experimental and Analysis Methods

In order to create a single-molecule particle tracking system for hM1AChR molecules, a cell model system was needed to ensure sufficient passage and overexpression of the hM1AChR gene. The human-embryonic kidney (HEK)-293 cells were used due to endogenous expression of hM1AChR. The conditions for cell culture used DMEM solution with sodium pyruvate, sodium chloride, 10% FBS and 1% P/S. Cells were placed in a 95% O₂ and 5% CO₂ incubation chamber for overnight storage and growth. In addition, cells were given no more than 72 hours to complete 80% confluency of a T-75 cm² flask before a new passage was created. Cells used for

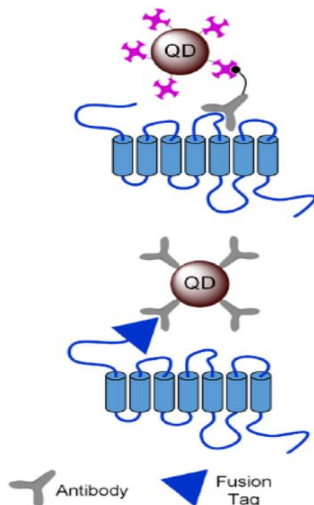


Figure 5. **Antibody-based single particle tracking of GPCRs.** from Kovton O. et al (2018)

experimentation went no further than an 18th passage. Preparation of cells for total internal reflection fluorescent (TIRF) imaging were grown over a 48-hour period. Roughly 24 hours into this growth, transient transfection of a hemagglutinin (HA)-fused hM1AChR gene was completed and cells were given another 24 hours to incubate to ensure full transfection of cells. After this process was completed, a two-step labeling method with biotinylated anti-hemagglutinin fragment was done on the day of TIRF microscopy imaging (Figure 5). For 15 minutes prior to imaging, 2 microliters of anti-hemagglutinin solution was added to the cell media and was allowed to incubate for this time period. After the 15 minutes have passed, the HEK-293 cells were washed twice with DMEM-Fluorobrite to wash away any cells that did not attach to the MATtek dishes and any cellular debris. After these washing, 2 mL of a 0.1 mM streptavidin-coated Qdot 605 nm solution was added and the cells were incubated for 5 minutes. After this time period passed, the cell dishes were washed twice more with DMEM-Fluorobrite to remove unattached Qdots to any receptors. For agonist-stimulated cells, an additional 5 minutes were given to incubate 0.1 mM solution of acetylcholine in biological-grade water. In order to

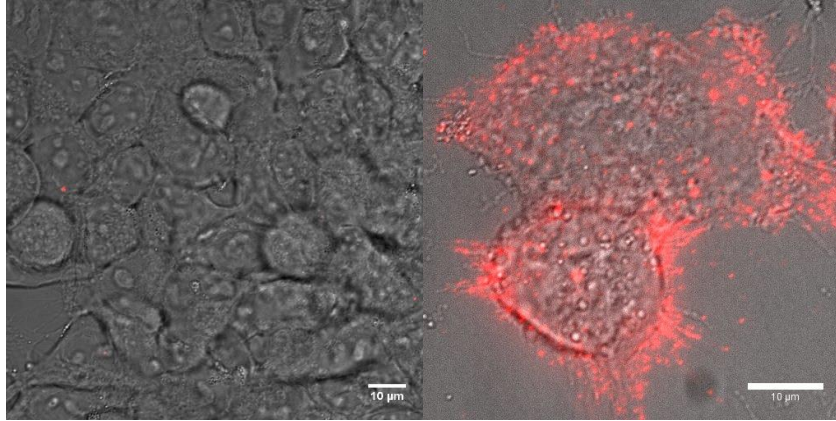


Figure 6. **Visualization of single hM1AChR molecules.** Left, basolateral image of HEK293 cells with no hM1AChR transfection. Right, basolateral image of HEK293 cells with hM1AChR transfection. Specific labeling is present along the cellular membrane after transfection.

visualize and track single Qdots, TIRF microscopy was used with a 488-nm laser at 50% capacity (Figure 6). In order to minimize the background noise presented with TIRF microscopy, a frame rate at 10-20 Hz was utilized. An autoexposure rate of 50-ms was applied to track and collected 1-min tracking windows for further analysis. After a 60-second time lapse was collected, further processing was done with the TrackMate plugin in ImageJ. The pixel width and height for each individual quantum dot was limited to 0.108 microns to avoid collection of aggregates for the analysis. Individual quantum dots were further detected by setting parameters of 0.5 microns as a diameter and a threshold value of 20 to include both dim and bright quantum dots presented per image. Individual trajectories were obtained by setting a linking max distance of 0.6 microns and a gap-closing max frame gap. Following all data processing for ImageJ, the 2-D positioning and time frame for each individual quantum dot were compiled in an Excel spreadsheet. After each data sample was collected, MATLAB programming was used to compile and formulate the necessary graphs and plots that will be presented in the results section.

Results & Discussion

Single hM1AChR proteins molecular dynamics were thoroughly analyzed through several mechanisms of action. At the basolateral membrane, these mechanisms included comparative diffusion coefficients through a cumulative distributive function plot, mean-squared displacement, and particle intensity. Data sets were compared between single proteins that were under basal conditions and proteins under agonist-stimulated conditions. It was expected that stimulation with acetylcholine would lower dynamic values as monomeric proteins would

aggregate and form oligomers. The data charts and graphs will provide larger context into how the diffusion dynamics of hM1AChR change with physiologically-relevant agonist-stimulated conditions in comparison to basal conditions. Once it was determined that the anti-HA QDot binding system was effective in detecting single hM1AChR, examination of alternate Qdot-to-receptor, such as conjugated ligands, was also performed. The candidate molecule, telenzepine, was selected based on its selective binding to hM1AChR and available conjugation sites to include an anchor structure optimal for performing cellular-based experiments. These charts aim to determine how a different targeting system potentially improves accurate data collection for hM1AChR physiological mechanisms. Using the anti-HA system, 650 trajectories were collected and analyzed for both conditions. The first mechanism investigated involved the measurement of cluster formation. The relevancy of this mechanism is thought to be related to high rates of physiological activity.

In all of these experiments, acetylcholine is used as the agonist. In a previous study, it was determined that oligomerization of individual hM1AChRs increases the chances of biological activity to take place. Therefore, it was determined that direct examination of Qdot-bonded hM1AChRs in conjunction with MATLAB programming could address this question.

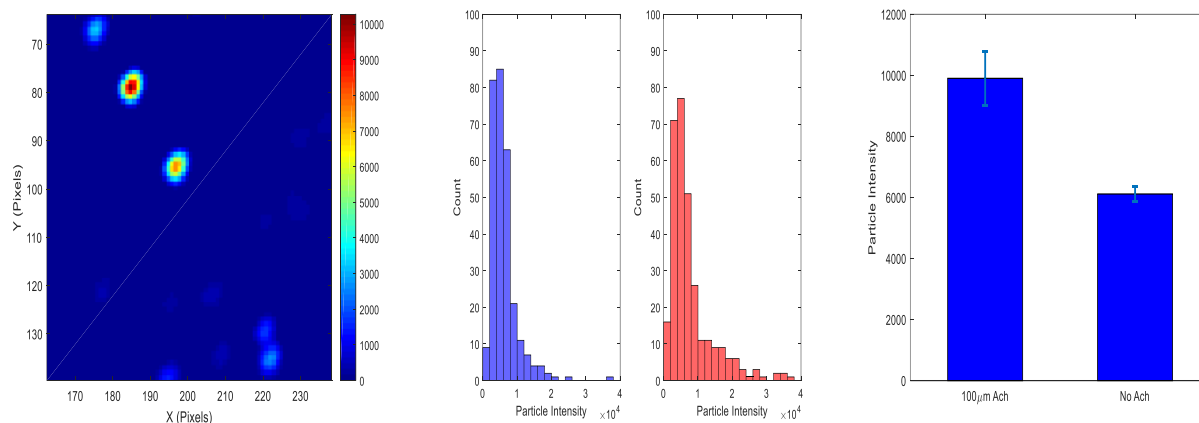


Figure 7. Analysis of cluster formation. Left, pixilation of concentration measurement of single hM1AChR, with red color featuring more concentrated areas and blue color less concentrated areas. Center, spread of particle intensity with blue bars identifying control environments and red bars identifying agonist-stimulated environments. Right, average cluster size with standard deviation included for both control and agonist-stimulated conditions.

The programming for this set of experiments took the relative intensities of individual receptors where more concentrated localizations appeared as a red-colored region and minimal receptor presence as blue-colored regions. A sample image is provided on the left panel of Figure 7, where a range of cluster groups can be seen. The clusters featuring more concentrated pixilation are of great interest as the greater number of these groups represent greater biological activity if presented in a more physiologically-relevant environment. The primary conclusions of these data sets show that hM1AChRs in acetylcholine-stimulated conditions not only feature a higher concentration of large cluster groups but also forms an average cluster size at least 1.5 times greater (intensity value increases to 9899 pixels from 6112 pixels under basal conditions) than receptors in a control environment to statistical significance ($p < 0.001$, Student's t-test). Although careful considerations need to be taken due to cells existing in an in-vitro environment rather than in-vivo, the results presented are promising in that we can predict enlarged cluster first being the molecular diffusion coefficient, and the second being the mean-squared

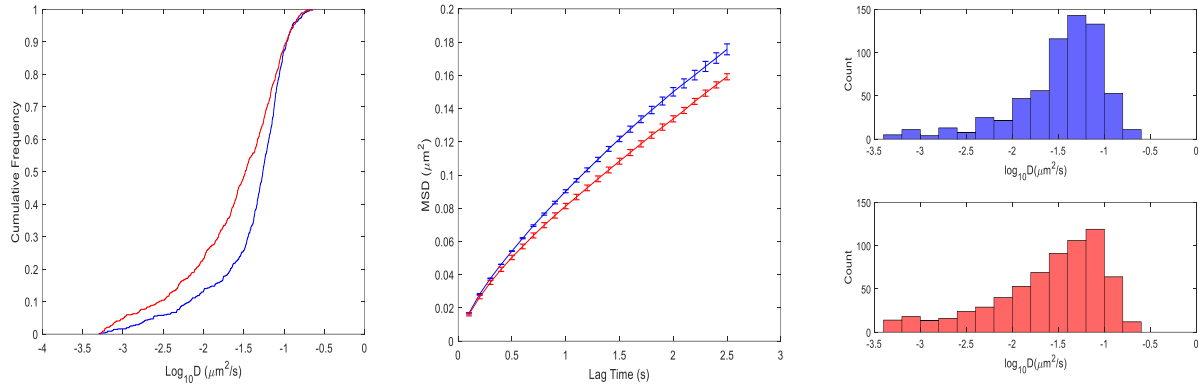


Figure 8. Lateral diffusion dynamics of hM1AChR. Left, molecular diffusion coefficients of both basal conditions (blue) and agonist-stimulated conditions (red). Center, mean-squared displacement of both conditions. Right, distribution of the molecular diffusion coefficients based on individual hM1AChR.

displacement for individual hM1AChR. The left panel provides the average diffusion coefficient through a cumulative distribution plot. This chart indicates that introducing acetylcholine stimulation decreases the average value (from $0.049 \mu\text{m}^2/\text{s}^2$ under basal conditions to $0.045 \mu\text{m}^2/\text{s}^2$) to statistical significance ($p < 0.001$ Kolmogorov-Smirnov test). Furthermore, the right panel provides the distribution of single hM1AChR coefficients in relation to the entire data set.

Ideally this distribution will identify whether hM1AChR exists in a single population pool or doubly populated featuring very quick and very slowing moving molecules. This information is important in detailing precise mechanisms for both extremes. For control conditions, there is one prominent collection of molecules moving at higher diffusion rates. However, under agonist-stimulated conditions, a growing secondary collection of slower-moving receptors is also present. The center panel of Figure 8 provides further analysis on the molecular dynamics of hM1AChR through its mean-squared displacement under both conditions. Further proof of decreased molecular movement via agonist stimulation is provided as there is a steady decrease in area covered over a set time period. These three panels should provide sufficient evidence that introduction of agonist stimulation lowers the lateral mobility of hM1AChR. This evidence can

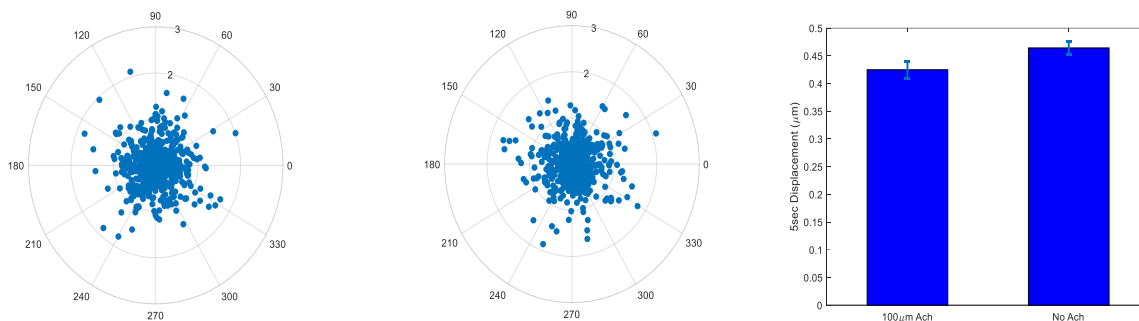


Figure 9. Polar scatter distribution of hM1AChR. Left, scatter of individual hM1AChR under control conditions. Center, panel scatter of individual hM1AChR under agonist-stimulated conditions. Right, average displacement with standard deviation included for both control and agonist-stimulated conditions.

be further linked to the increased clustered formation during agonist-stimulation as a potential reason for these slower moving populations. The final mechanism of interest was the instantaneous radial displacement of hM1AChR. Figure 9 details the distribution based on the relative distance traveled for individual receptors after 5 seconds at the start of 1-min tracking period. The left and center panels detail the radial distribution of hM1AChR during control and agonist-stimulated conditions respectively. Further investigation on the average distance based on the condition shows that after stimulation with acetylcholine there is a small decrease in distance traveled (from 0.049 μm under basal conditions to 0.046 μm) to statistical significance ($p < 0.05$, Student's t-test).

Overall, the three primary mechanisms targeted show that when stimulated with acetylcholine, hM1AChR on average will feature decreased dynamics and a greater tendency to form larger clusters. Based on information provided earlier, these appear to be appropriate conclusions as oligomerization of individual receptors is more likely to activate biological activity with hM1AChR. After successful investigation of predicting and determine the molecular mechanisms of hM1AChR under control and agonist-stimulated environments with an N-terminus antibody attachment, a secondary interest involved using a ligand-based approach using

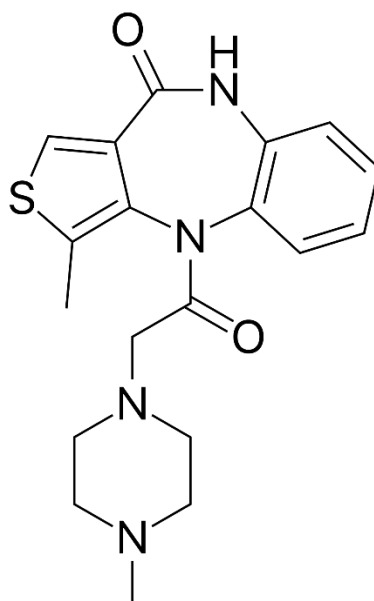


Figure 10. **Schematic structure of telenzepine.**

molecules with great specificity to hM1AChR. The primary molecule of interest that fits this goal is telenzepine (Figure 10). This compound has not only been shown to have high selectivity of hM1AChR in comparison to its other subtypes, it contains a suitable site for conjugation to optimize attachment of a quantum dot to an allosteric binding site to the receptor.¹⁹ Figure 11 presents the schematic of the first attempted ligand conjugate of telenzepine, IDT791. This ligand is composed of a hydrophobic region ideal for minimal interaction detrimental to the tracking experiment with the equally hydrophobic cellular membrane. Attached directly to this hydrophobic region is a PEGylated spacer region that allows for stability of the ligand in the hydrophilic extracellular environment. This group also features a solidly rigid structure that will minimize movement of the Qdot not innate with movement of the receptor itself. And lastly, the biotin group attached to the end of the ligand will maximize attachment to the quantum dot itself,

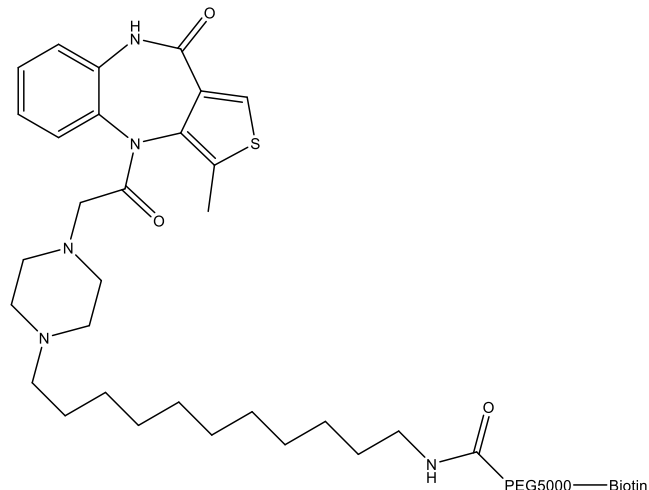


Figure 11. **Schematic structure of IDT791.**

as seen with the antibody group. The primary experiments with the ligand involve an initial screening that will hopefully show the selectivity to single hM1AChR equivalent with the primary anti-HA-Qdot system. Using this ligand-based approach with IDT-791, the primary experiments aimed to determine whether quantum dots could attach to the ligand, and if so, where they able to detect to singular hM1AChR molecules. The set-up of these experiments included taking spinning disk confocal microscopy images on basolateral and cross-section levels. Figure 12 includes a negative-control experiment to determine an estimated amount of ligand plate-binding. Too much binding will limit the analysis that can be obtained as single molecules will either not be detected or become confused with aggregate protein formation. Close examination of this figure gives two immediate conclusion concerning ligand-binding to the HEK-293 cells. The first conclusion given is that a tremendous amount of plate-binding renders single analysis to be incredibly ineffective in the event of successful IDT-791 binding to hM1AChR. The second conclusion takes aim at the cross-sectional images, which aim to determine whether the ligand is capable of binding to the cells without particular specificity. As there is no transfection with hM1AChR present with these cells, it was worth of interest to

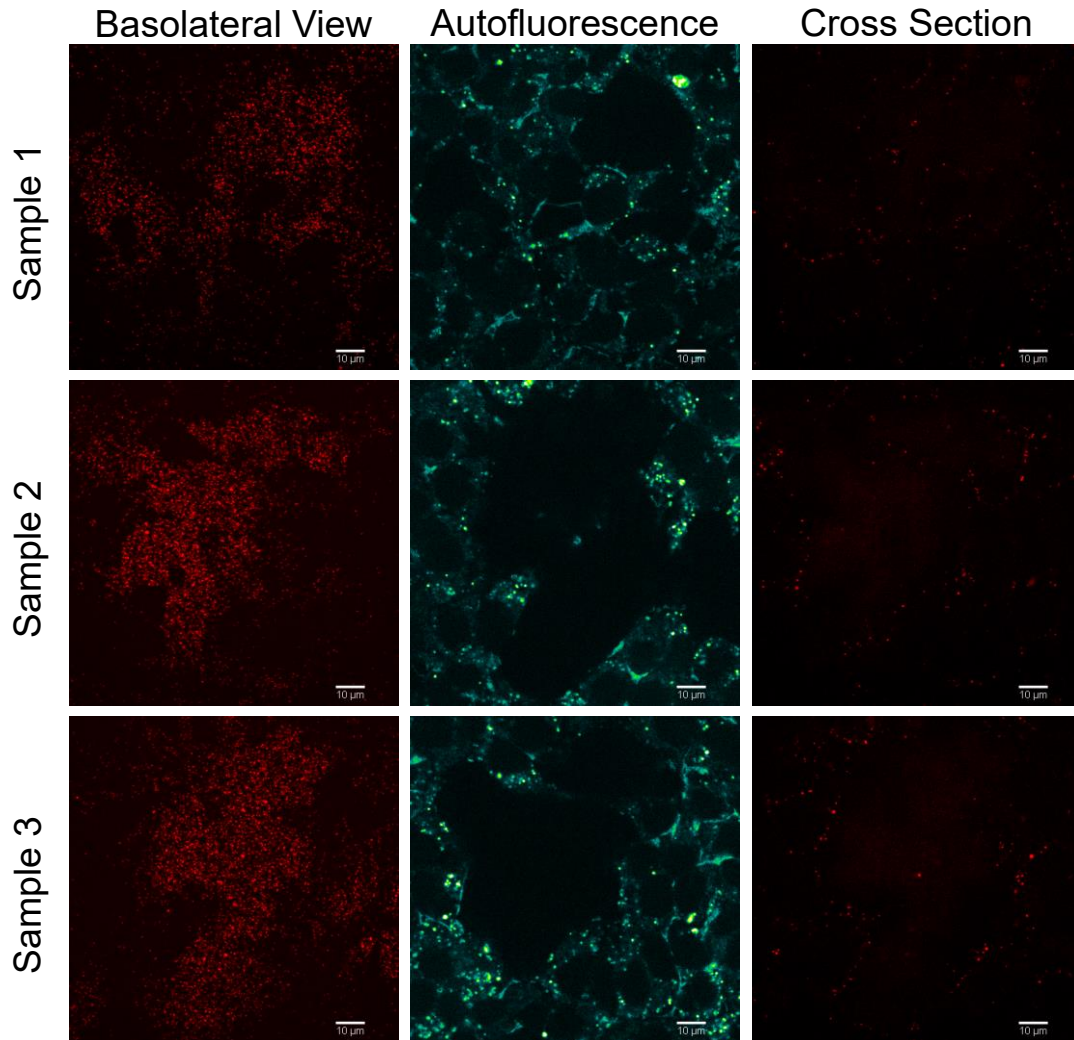


Figure 12. **Molecular screening of Qdot-bonded IDT791 to HEK-293 cells with no transfection of hM1AChR.** Left, Spinning-disk microscopy imaging of HEK-293 cells on basolateral plane. Center, autofluorescence of HEK-293 cells on basolateral plane. Right, spinning disk microscopy imaging of HEK-293 cells on cross section plane.

determine a baseline of any particular quantity of cellular binding to predict the ratio of hM1AChR specific binding and non-specific binding. A heavy presence of the latter will lead to undesirable results as there will be no sure way to tell if data collection will be accurate. Figure 13 features cells with hM1AChR transfection to tell if the transfection will decrease the plate binding seen earlier and increase more binding to the cell. Initial conclusions indicate that there is not a significant decrease in plate binding, but what is featured is a steady increase of cell

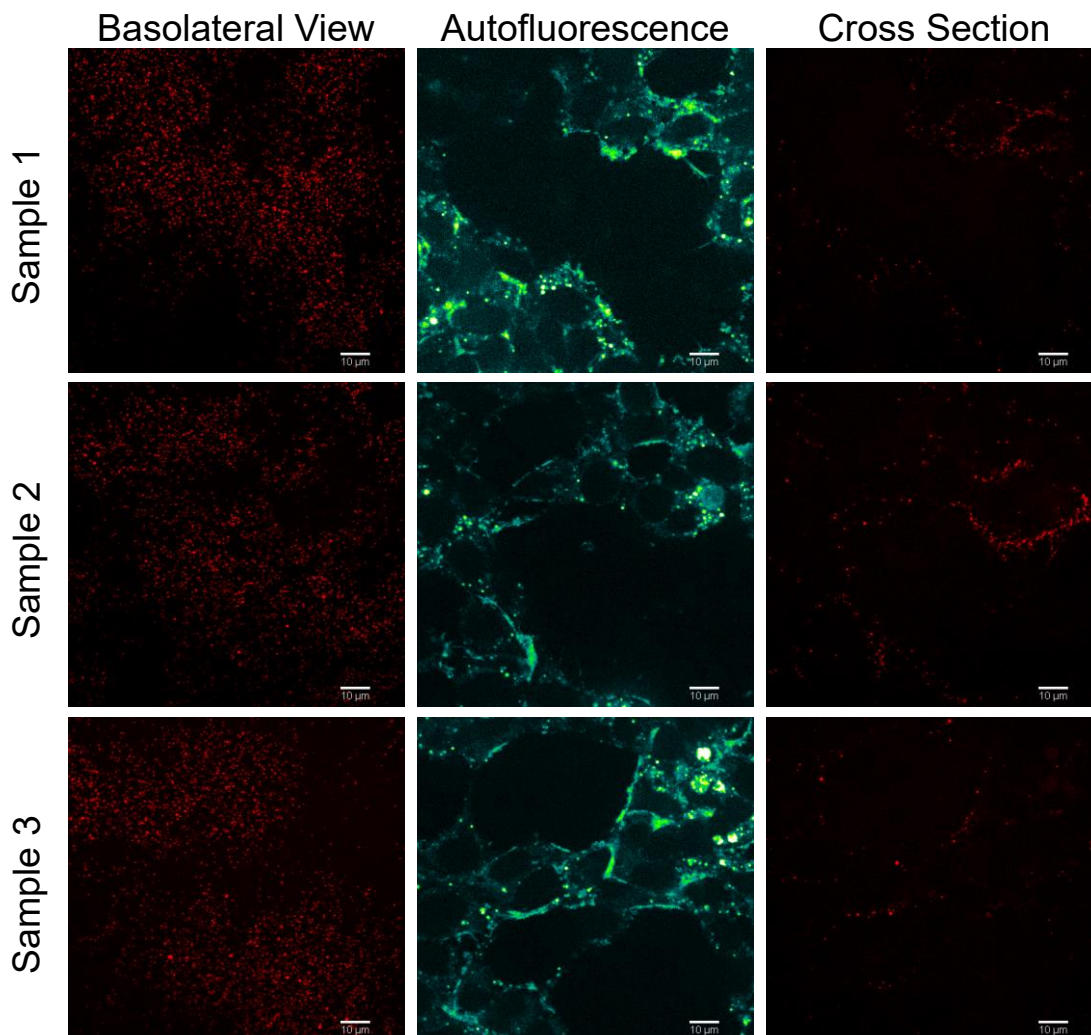


Figure 13. **Molecular screening of Qdot-bonded IDT791 to HEK-293 cells with transfection of hM1AChR.** Left, Spinning-disk microscopy imaging of HEK-293 cells on basolateral plane. Center, autofluorescence of HEK-293 cells on basolateral plane. Right, spinning disk microscopy imaging of HEK-293 cells on cross section plane.

binding. No further studies were performed however due to significant non-specific binding on the basolateral membrane. Without a comparable amount of specific binding equivalent to the antibody system, there will be no reliable statistics that can compare the molecular dynamics of both systems. The undesirable results with IDT791 lead to creation of a new telenzepine-derived ligand titled IDT974 (Figure 14). What differentiates this ligand from IDT791 is the removal of the lengthy alkyl chain and exchanged with a much shorter benzyl chain as the hydrophobic

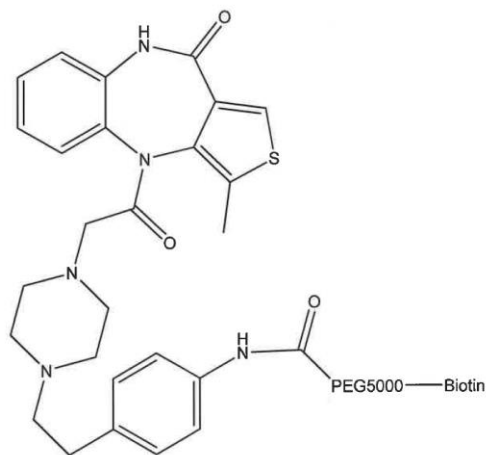


Figure 14. **Schematic structure of IDT794.**

region. Given a new region to minimize reaction with the cellular membrane, the primary purpose of screening this ligand was to determine whether there would be less non-specific binding to the plate. The next two figures will strictly determine the success or failure of this new ligand to primarily attach to hM1AChR transfected cells.

New images were performed with TIRF microscopy to better replicate and compare to the earlier experiments featuring the antibody system. As performed with IDT791, basolateral images were taken to not only look for heavy plate binding with non-transfected HEK293 cells, but also a greater amount of specific binding to hM1AChR transfected cells. Figure 15 features non-transfected cells as another baseline test to not only look at whether there was any non-specific labeling to cells but also a general look at the amount of plate binding. The side-by-side panel aimed to determine whether the quantum-dots present were attached to the cellular membranes of any cells present. Comparing the presence of quantum dots with the DIC images, there appears to be little cellular binding as predicted in addition to a decreased amount of plate binding. However, there is not much conclusive evidence to determine whether the quantum dots

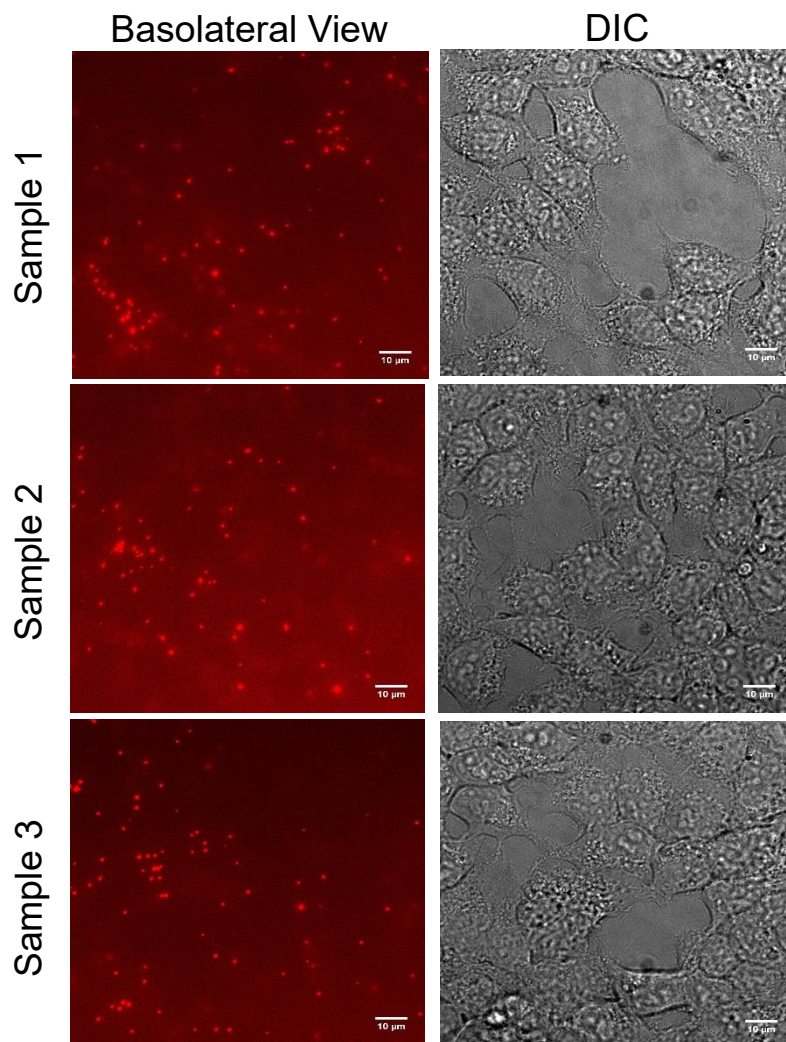


Figure 15. **Molecular screening of Qdot-bonded IDT794 to HEK-293 cells with no transfection of hM1AChR.** Left, TIRF microscopy imaging of HEK-293 cells on basolateral plane. Right, DIC microscopy imaging of HEK-293 cells on basolateral plane.

detected are strictly adhered to the plate or potentially attached to cells. With the previous dilemma presented, it was with great interest to test IDT794 binding to cells transfected with hM1AChR in hopes of not only less plate binding, but specific binding to the HEK293 cells as well. Figure 16 presents this answer with a repeated set of experiments identical to the previous set of conditions. The side-by-side images prevent little improvement with what appears to be a good deal of plate binding. However, there does seem to be some steady labeling along the cellular membranes in a handful of cells. With the experimentation of two ligands designed to

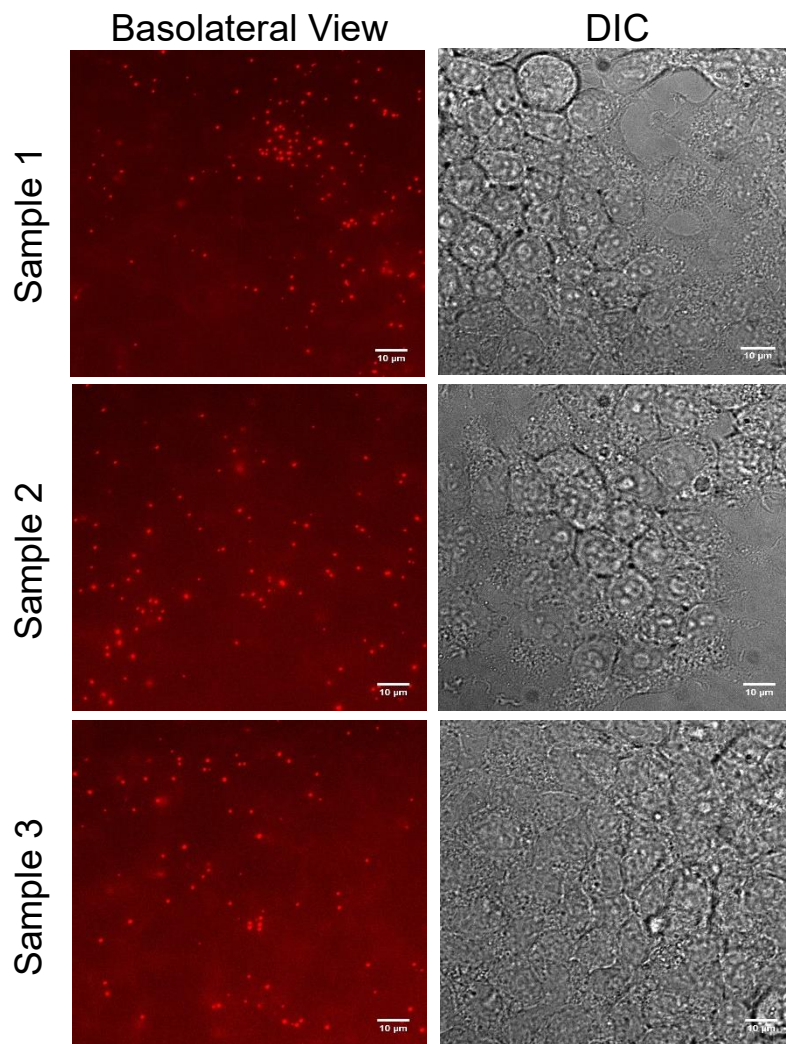


Figure 16. **Molecular screening of Qdot-bonded IDT794 to HEK-293 cells with transfection of hM1AChR.** Left, TIRF microscopy imaging of HEK-293 cells on basolateral plane. Right, DIC microscopy imaging of HEK-293 cells on basolateral plane.

specifically label hM1AChR, there does not appear to be much success with either one. However, the redesign via IDT794 shows significantly less plate binding, although not necessarily increasing an adequate amount of cellular labeling. While there was no incredible success in creating a suitable ligand for direct comparison to the earlier antibody system, there does appear to be a good template for future ligand design. It appears that future optimization of the hydrophobic region will likely to further decrease the presence of plate binding in hope for a

greater amount of specific labeling to produce a working ligand-to cell-targeted system to replicate and potentially improve the results of the successfully created antibody targeted system.

Conclusions

With the steady population of patients with mental health disorders and a limited amount of adequate treatment options, it has become imperative to find new methods to develop more efficient medication to combat this issue. In order to develop a more complete understanding on the molecular mechanisms of one prominent target for mental health treatment, hM1AChR, the development of a Qdot targeted system has been completed. The aim of this work had three primary goals. The first goal concerned the identification of single hM1AChR with quantum-dot nanotechnology, the second was to determine underlying mechanisms of this protein, and the third explored alternate option of specific targeting of the receptor.

The majority of the experiments took place through the creation of an anti-HA tag connected to a N-terminus HA-fused tag on hM1AChR. This system was effective in targeting single hM1AChR proteins transfected into HEK293 cells with quantum dots that aided with the visualization of these receptors via TIRF microscopy. The use of ImageJ and MATLAB programming allowed for single proteins to be analyzed for a number of dynamic mechanisms in order to gain a more complete analysis of hM1AChR activity than previous studies have provided. The decision to include conditions with agonist stimulation aimed to represent the receptor into an environment where simulated biological activity can take place. Although these experiments were limited to in-vitro environments, it is with hope that these studies and analyzes will translate well into more physiological relevant environments.

Three dynamics mechanisms were looked at in order to provide preliminary insight on the innate quantities of hM1AChR in both control and agonist-stimulated environments. The first unit looked into cluster formation, which indicates a sign of higher chances for biological activity to take place. It was predicted beforehand that stimulation with acetylcholine will recruit monomeric receptors to create larger clusters to simulate protein activation in preparation for physiological activity. The results of this experiments were significant and met the expectations of an increase of the average cluster size of acetylcholine-stimulated hM1AChR in relation to the control environment. More studies were determined to create a bigger picture of overall hM1AChR movement on a more precise individual level.

This level of study was achieved by looking at two more units of molecular dynamics. The first was determining the diffusion coefficients of single hM1AChR both in control and acetylcholine-stimulated environments. There was significant evidence to see how the introduction of acetylcholine to activate hM1AChR slows down the diffusion dynamics. A further look into the distribution of molecular movement shows that while there is a steady population of faster moving receptors in a control environment, stimulation with acetylcholine presents two steady populations, including one with a significant increase in slower moving receptors that could indicate the increased average cluster size shown earlier. The next evidence of agonist-stimulation effects is seen in a mean-squared displacement chart, where acetylcholine stimulation decreases the molecular area distance traveled per receptor over a steady time period. The final plots included for this section of experiments is a polar scattered plot to look more into the instantaneous distance traveled when data collection is started for each receptor. This data supports the earlier results by showing a decrease in average distance per distance after acetylcholine stimulation.

The collective results of comparing the molecular dynamics of hM1AChR repeatedly support the notion that a simulated environment aimed to induce biological activity via acetylcholine stimulation decreases several units of lateral mobility. In addition to previous studies providing insight on individual receptor quantitative analysis, the addition of a more reliable fluorescence source with quantum dots and providing results on acetylcholine-stimulated hM1AChR help further the knowledge on the innate properties of this receptor.

The second portion of this study looked into alternative targeting methods using a ligand-based probe, replacing the antibody-based system. A successful ligand capable of binding to the receptor of interest and a quantum dot required several components: a highly-selective compound capable of binding to hM1AChR, a hydrophobic region to minimize negative interaction with the cellular membrane, a hydrophilic spacer for stability in the hydrophilic extracellular environments, and biotin to bind to the quantum dot.

The first attempt of creating an appropriate ligand was IDT791, a telenzepine-based molecule with the end conjugated with the previously mentioned components. While there was promising evidence of cellular binding to the hM1AChR transfected cells, there was a significant amount of plate-binding that rendered the target system to be unreliable. The second attempt included another telenzepine-based ligand with an exchanged hydrophobic region named IDT794. This ligand featured less plate binding and a roughly equal amounts of cellular binding. Unfortunately, the system once again is proven unreliable due to non-specific labeling on both the plates and the cells. Further experimentation should be able to provide a comparable system to the antibody-based system capable of producing similar or potentially improved results concerning hM1AChR mobility. Multiple drug candidates that have various direct influence on hM1AChR activation can provide intriguing new insights that could further support the primary

conclusions produced from this study.^{20,21} In addition, new recent discoveries based on hM1AChR post-modifications via various ligand binding will influence future in how the receptor can be studied with the newly produced Qdot-to-receptor system.²²

With all of the presented data, it has been demonstrated than an improved system for labeling individual hM1AChR proteins provides additional important insight on the molecular mechanisms in both controlled and agonist stimulated conditions. It is with hope that even more information can be acquired for relevant-mutated hM1AChR proteins to provide a larger picture to target new developments for mental health treatments.

References

- (1) Yamasaki M. et al (2010) Preferential localization of muscarinic M1 receptor on dendritic shaft and spine of cortical pyramidal cells and its anatomical evidence for volume transmission. *J. Neurosci.* 30, 4408–4418.
- (2) Roth TC. et al (2018) Of molecules, memories and migration: M1 acetylcholine receptors facilitate spatial memory formation and recall during migratory navigation. *Proc. R. Soc. B* **285**, 1-7.
- (3) Medeiros R. et al (2011) Loss of Muscarinic M1 Receptor Exacerbates Alzheimer's Disease–Like Pathology and Cognitive Decline. *Am. J. Pathol.* **179**, 980-991.
- (4) Lebois E.P. et al (2017) Disease-Modifying Effects of M1 Muscarinic Acetylcholine Receptor Activation in an Alzheimer's Disease Mouse Model. *ACS Chem. Neurosci.* 8, 1177-1187.
- (5) Espinoza-Fonseca L.M. et al (2008) Structure and dynamics of the full-length M1 muscarinic acetylcholine receptor studied by molecular dynamics simulations. *Archives of Biochemistry and Biophysics* 469, 142–150.
- (6) Uwada J. et al (2014) Intracellular localization of the M1 muscarinic acetylcholine receptor through clathrin-dependent constitutive internalization is mediated by a C-terminal tryptophan-based motif. *J. Cell Sci.* 127, 3131-3140.
- (7) Halls M.L. et al (2016) Plasma membrane localization of the μ -opioid receptor controls spatiotemporal signaling. *Sci.* 9, 1-13.
- (8) Calebiro D. et al (2013) Single-molecule analysis of fluorescently labeled G protein-coupled receptors reveals complexes with distinct dynamics and organization. *PNAS* 110, 743-748.
- (9) Thal DM. et al (2016) Crystal structures of the M1 and M4 muscarinic acetylcholine receptors. *Nature* **531**, 335-340.
- (10) Peng J.Y. et al (2006) The predicted 3D structures of the human M1 muscarinic acetylcholine receptor with agonist or antagonist bound. *ChemMedChem* 1, 878–890.
- (11) Stewart A. et al. (2012) RGS proteins in heart: brakes on the vagus. *Front. Physiol.* **3**, 1-14.
- (12) Vijayraghavan S. et al (2018) Muscarinic M1 receptor overstimulation disrupts working memory activity for rules in primate prefrontal cortex. *Neuron* 98, 1-13.
- (13) Calabresi P. et al (1999) Activation of M1-like muscarinic receptors is required for the induction of corticostriatal LTP. *Neuropharmacology* 38, 323–326.

- (14) Gurwitz D. et al (1994) Discrete activation of transduction pathways associated with acetylcholine M1 receptor by several muscarinic ligands. *Eur. J. Pharmacol.* 267, 21-31.
- (15) Hern JA. et al (2010) Formation and dissociation of M1 muscarinic receptor dimers seen by total internal reflection fluorescence imaging of single molecules. *PNAS* 107, 2693-2698.
- (16) Moller T.C. et al (2018) Oligomerization of a G protein-coupled receptor in neurons controlled by its structural dynamics. *Sci. Rep.* 8, 1-15.
- (17) Ilien B. et al (2009) Pirenzepine promotes the dimerization of muscarinic M1 receptors through a three-step binding process. *J. Biol. Chem.* 284, 19533–19543.
- (18) Kovton O et al (2018) Single quantum dot tracking illuminates neuroscience at the nanoscale. *Chem. Phys. Lett.* **706**, 741-752.
- (19) Schudt C. et al (1988) Does the prolonged occupancy of M1 receptors by telenzepine protect them against the action of vagally released acetylcholine? *Pharmacol.* 37, 32-39.
- (20) Pediani J.D. et al (2016) Dynamic regulation of quaternary organization of the M1 muscarinic receptor by subtype-selective antagonist drugs. *J. Biol. Chem.* 291, 13132-13146.
- (21) Thorn C.A. et al (2019) Striatal, hippocampal, and cortical networks are differentially responsive to the M4- and M1-muscarinic acetylcholine receptor mediated effects of xanomeline. *ACS Chem. Neuro.* 10, 1753-1764.
- (22) Xu J. et al (2019) Direct SUMOylation of M1 muscarinic acetylcholine receptor increases its ligand-binding affinity and signal transduction. *FASEB J.* 33, 3237-3251.